Electronic Supplementary Material (ESI) for Journal of Materials Chemistry A.

Electronic Supplementary Information

Flexible coaxial fiber-shaped asymmetric supercapacitors based on manganese, nickel co-substituted cobalt carbonate hydroxides

Xueying Cao[a,b†], Ying Liu[a†], Yuxue Zhong[a], Liang Cui[b*], Aitang Zhang[a], Joselito M. Razal[c], Wenrong Yang[d], Jingquan Liu[a,b*]

[a]College of Material Science and Engineering, Institute for Graphene Applied Technology Innovation, Qingdao University, Qingdao 266071, PR China.

[b]College of Material Science and Engineering, Linyi University, Linyi, 276000, PR China.

[c]Institute for Frontier Materials, Deakin University, Geelong, Victoria 3216, Australia.

[d]School of Life and Environmental Sciences, Deakin University, Victoria 3217, Australia.

† Xueying Cao and Ying Liu contributed equally to this work.

E-mail: clzkzy@163.com; jliu@qdu.edu.cn.

Calculations:

The normalized volumetric capacitance C_v (F cm^{-3}) derived from galvanostatic discharge (GCD) curves were calculated according to the following equation:

$$C_v = \frac{I\Delta t}{V\Delta U}$$

Where I (A) is the discharge current, Δt (s) is the discharge time, ΔU (V) is the potential window and V is the total volume of the whole device (cm^3).

The volumetric energy densities (E) and power densities (P) of the device were calculated by following equations:

$$E = \frac{1}{2} C_v \Delta U^2$$

$$P = E/\Delta t$$

Where E (mWh cm^{-3}) represents volumetric energy densities; C_v (F cm^{-3}) is the volumetric capacitance; ΔU (V) is the voltage operation window; P (W cm^{-3}) represents power density.

The normalized areal capacitance C_A (F cm^{-2}) derived from GCD curves were calculated according to the following equation:

$$C_A = \frac{I\Delta t}{A\Delta U}$$

Where I (A) is the discharge current, Δt (s) is the discharge time, ΔU (V) is the potential window and A (cm^2) is the total area of the two electrode active materials in the whole device.

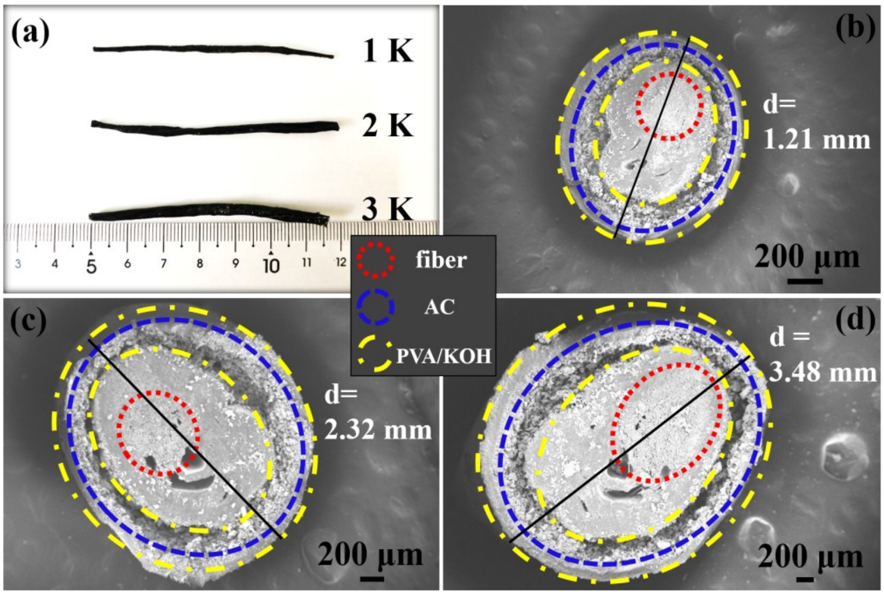

Fig. S1 (a) Photograph of FASCs with different amounts of carbon fibers. SEM images of FASC cross sections of the device with (b) 1 K (c) 2 K and (d) 3 K carbon fibers.

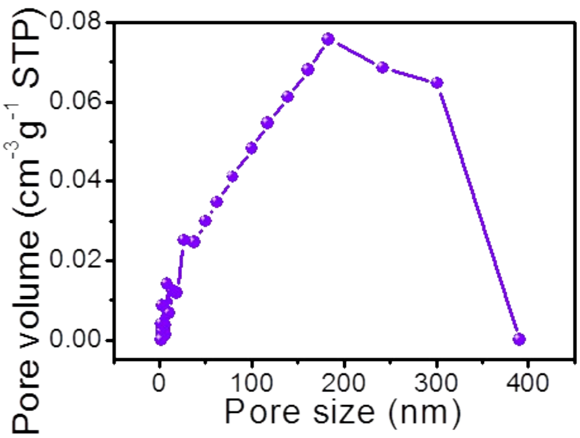

Fig. S2 The pore-size distribution for MnNiCo-CH/CF sample.

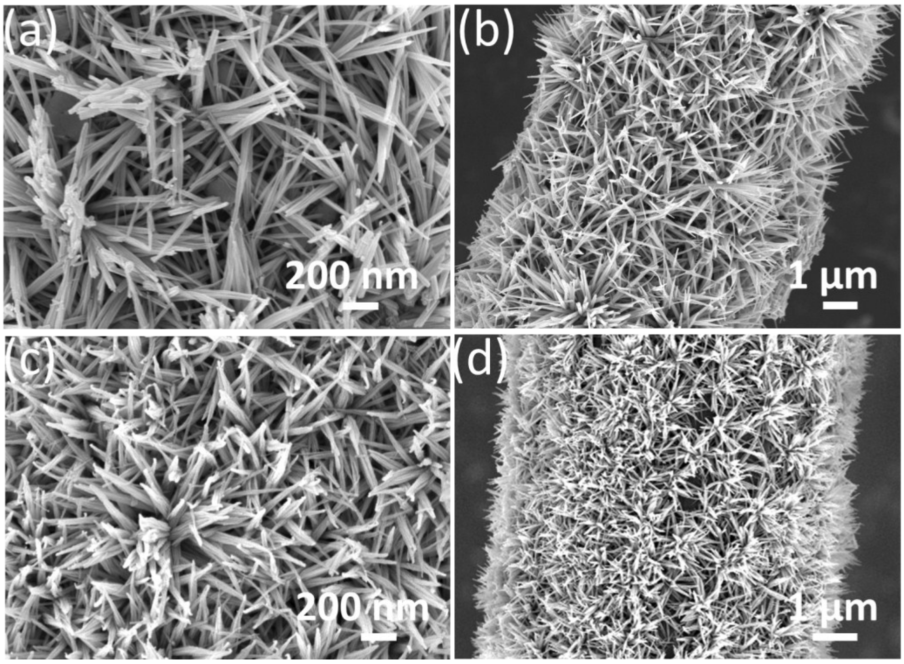

Fig. S3 SEM images of (a, b) NiCo-CH/CF and (c, d) Co-CH/CF.

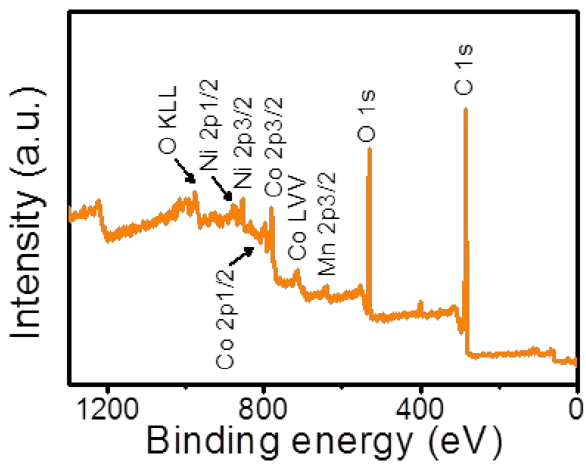

Fig. S4 XPS survey spectrum of MnNiCo-CH.

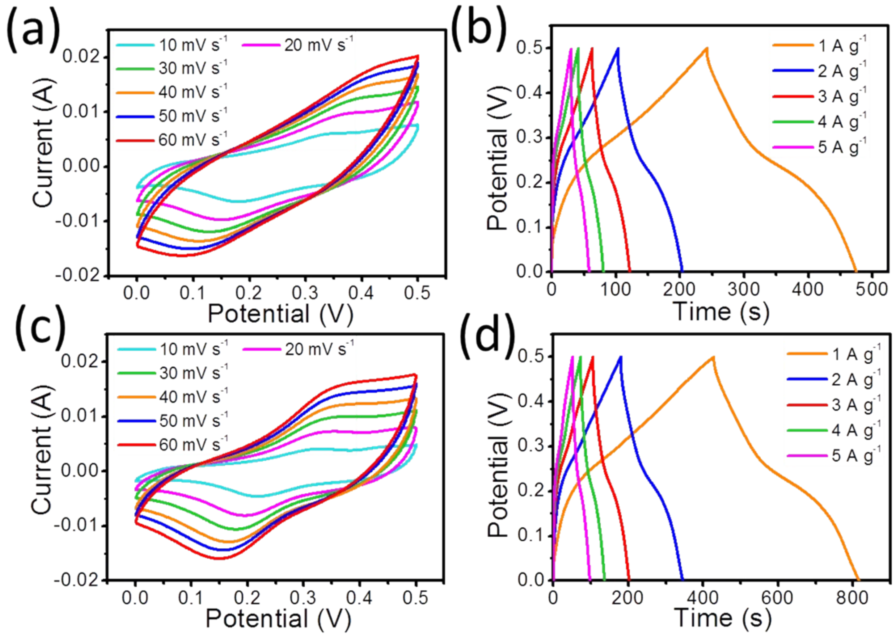

Fig. S5 (a) CV curves and (b) GCD curves of the Co-CH/CF electrode at various scan rates and different current densities. (c) CV curves and (d) GCD curves of the NiCo-CH/CF electrode at various scan rates and different current densities.

The contribution of capacitive effect can be determined by plotting log oxydic and reduced peaks currents (I) versus log scan rates (v). According to a power-law relationship with the sweep rate v (mV s^{-1}):[1]

$$I = av^b$$

where a and b are adjustable values, b = 1 indicates a capacitive process, and b = 0.5 indicates a semi-infinite diffusion process.

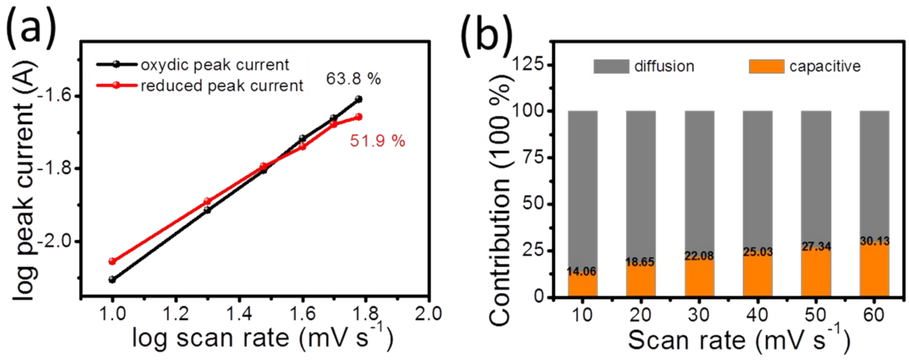

Fig. S6 (a) Relationship between logarithm peak currents and logarithm scan rates of MnNiCo-CH/CF electrode. (b) Capacitive and diffusion contribution ratio of capacitance of MnNiCo-CH/CF electrode at various scan rates.

As shown in Fig. S6a, the b-value for MnNiCo-CH/CF electrode is 0.58 at the scan rates between 10 and 60 mV s^{-1}, suggesting both capacitive and battery behaviors are existent in MnNiCo-CH/CF electrode.[2] The capacitive contribution can be calculated by a current response (I) at a fixed potential (U) according to the following equation:

$$I(U) = k_1 v + k_2 v^{1/2}$$

where $k_1 v$ namely capacitive effects and $k_2 v^{1/2}$ namely diffusion-controlled insertion, which belongs to faradaic contribution, k_1 and k_2 can be calculated from the slope and the y-axis intercept point of a straight line.

As shown in Fig. S6b, with the scan rates increasing, the capacitive contribution in MnNiCo-CH/CF electrode is gradually improving, but still occupies a small portion about 30 %, which confirms the coexistence of capacitive and battery behaviors and the leading roles of faradaic contribution.

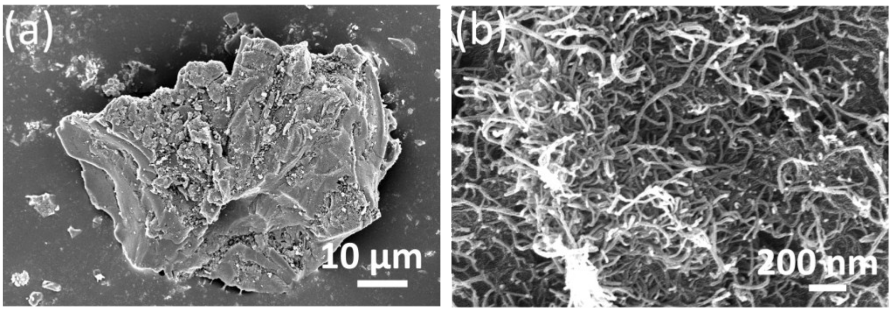

Fig. S7 SEM images of (a) AC and (b) CNTs.

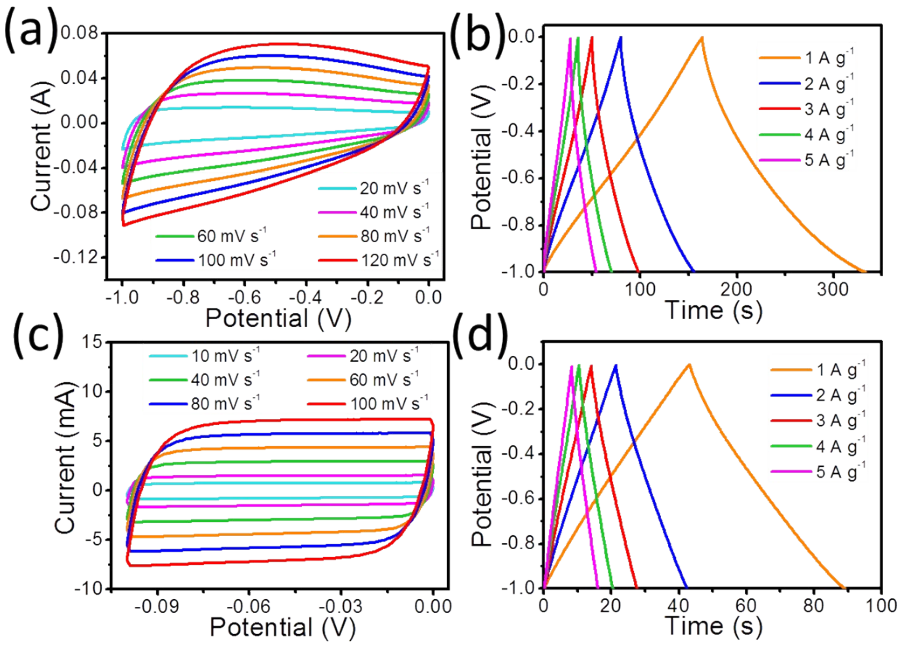

Fig. S8 (a) CV curves and (b) GCD curves of the AC electrode at various scan rates and different current densities. (c) CV curves and (d) GCD curves of the CNTs electrode at various scan rates and different current densities.

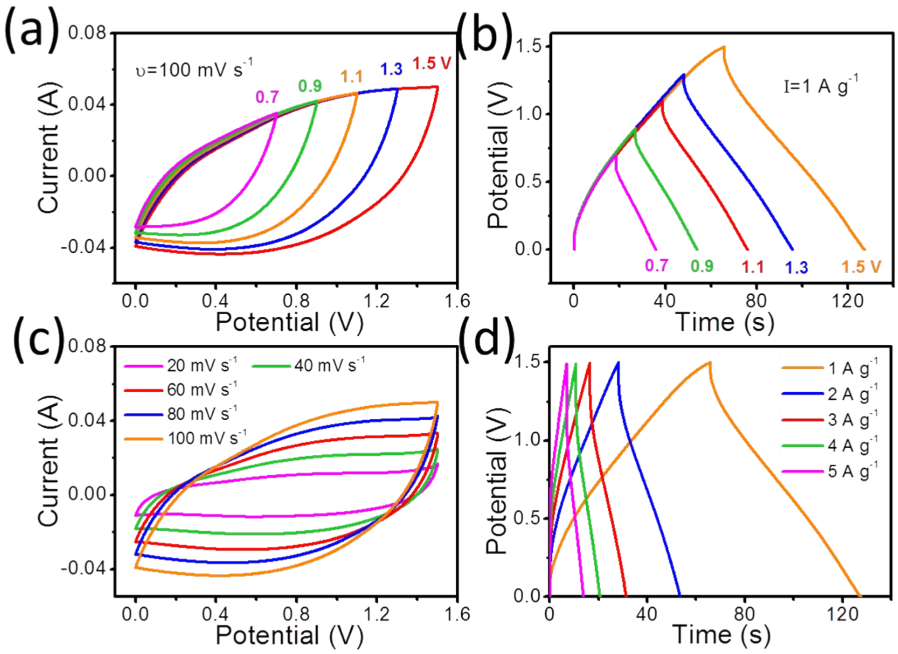

Fig. S9 Electrochemical performance tests for MnNiCo-CH/CF//CNTs ASC: (a) CV curves in different potential ranges at a scan rate of 100 mV s^{-1}. (b) GCD curves in different potential ranges at a current density of 1 A g^{-1}. (c) CV curves and (d) GCD curves at various scan rates and different current densities.

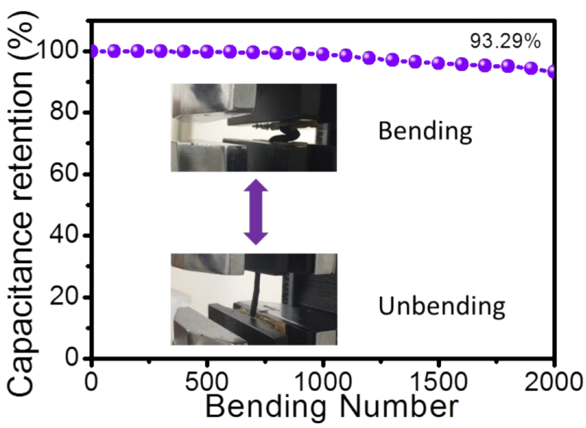

Fig. S10 The bend cycle stability of assembled FASC device.

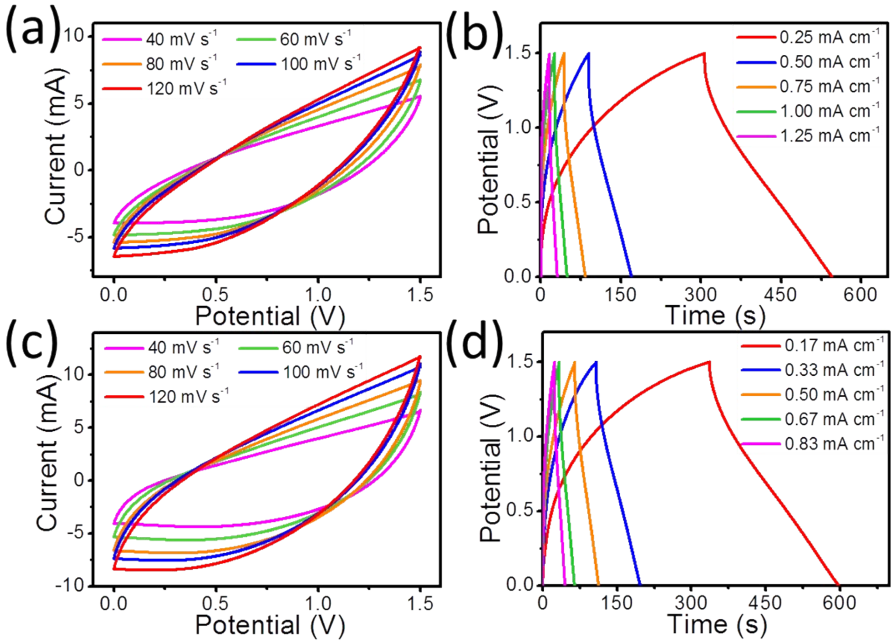

Fig. S11 (a) CV and (b) GCD curves of the FASC device with a length of 4 cm at various scan rates and current densities. (c) CV and (d) GCD curves of the FASC device with a length of 6 cm at various scan rates and current densities.

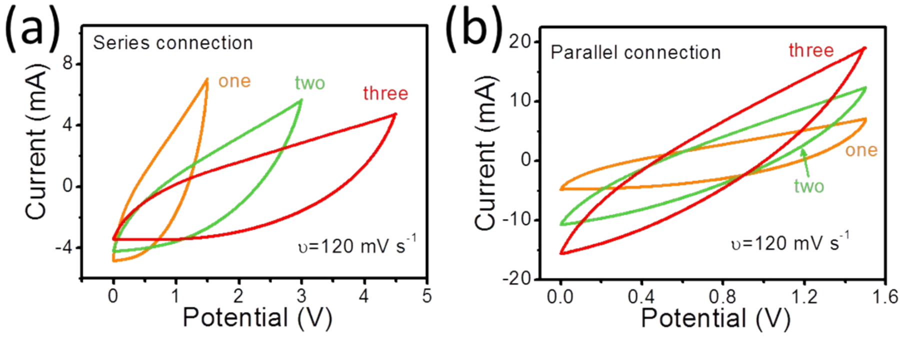

Fig. S12 CV curves for FASC devices connected in (g) series and (h) parallel.

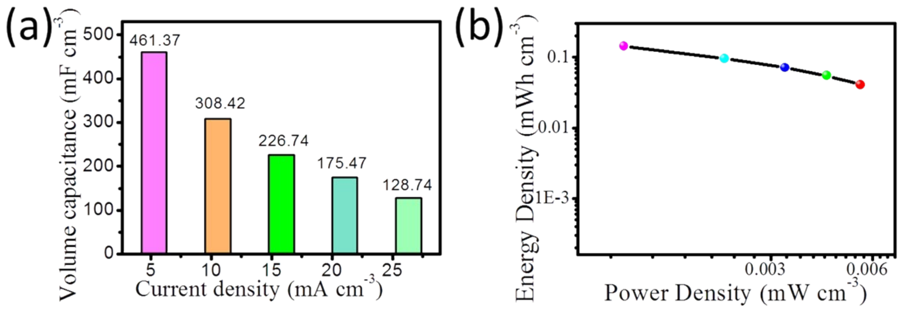

Fig. S13 The normalized volumetric (a) capacitance and (b) energy/power densities of FASC device.

Table S1 The areal and volumetric specific capacitances as well as length capacitances of the as-assembled FASCs at different current densities.

I (mA cm^{-1})	0.5	1.0	1.5	2.0	2.5
C_l (mF cm^{-1})	43.83	29.30	21.54	16.67	12.33
I (mA cm^{-2})	0.46	0.92	1.37	1.83	2.29
C_A (mF cm^{-2})	40.14	26.83	19.73	15.27	11.20
I (mA cm^{-3})	5.26	10.53	15.79	21.05	26.32
C_V (mF cm^{-3})	461.37	308.42	226.74	175.47	128.74

Table S2 The comparison of electrochemical performances of our assembled coaxial fibre-based supercapacitors with other coaxial or fiber-based supercapacitors reported recently.

Electrode material	**Electrolyte Voltage (V)**	C_s **(F g^{-1})**	C_A **(mF cm^{-2})**	C_l **(mF cm^{-1})**	**Cycle life**	**Ref.**
MnNiCo-CH/CF//AC	1.5	93.13	40.14	43.83	83.86% for 8000 cycles	This work
MnNiCo-CH/CF//CNTs	1.5	41.20	—	—	—	This work
MWCNTs/CMF	1.0	—	71.1	5.1	94% for 1000 cycles	3
Hollow RGO/PEDOT	0.7	63.1	304.5	8.1	96% for 10000 cycles	4
Chinese ink/AC	0.8	—	3.18	0.1	—	5
MnO_2-CNT-G-Ni	0.8	—	31	9.93	82% for 10000 cycles	6
Chinese ink/Chinese ink	1.0	—	11.2	0.3	86% for 1500 cycles	7
Ink on fiber/Ink on fiber	0.8	—	26.4	0.504	robust after 15000 cycles	8
Ti wire/MWCNT	0.6	—	—	0.077	—	9
RGO/Ni cotton	0.8	311	—	110	82% for 10000 cycles	10
CNT/PANI	1.0	215.6	—	—	69% for 1000 cycles	11
CNT@PANI/CNT@PANI	0.8	—	38	—	91% for 800 cycles	12

CNT@Co_3O_4/CNT@Co_3O_4	0.8	87.6	52.6	—	91% for 1000 cycles	13
CNT@NiO/CNT@NiO	0.8	25.9	15.2	—	94% for 1000 cycles	13

References

1 O. Yu, R. Huang, X. Xia, H. Ye, X. Jiao, L. Wang, W. Lei, Q. Hao, *Chem. Eng. J.,* 2018, **355,** 416-427.

2 T. Brezesinski, J. Wang, S. H. Tolbert, B. Dunn, *Nat. Mater.,* 2010, **9,** 146-151.

3 L. Viet Thong, K. Heetae, G. Arunabha, K. Jaesu, C. Jian, V. Quoc An, P. Duy Tho, L. Ju Hyuck, K. Sang-Woo, L. Young Hee, *ACS Nano,* 2013, **7,** 5940-5947.

4 G. Qu, J. Cheng, X. Li, D. Yuan, P. Chen, X. Chen, B. Wang, H. Peng, *Adv. Mater.,* 2016, **28,** 3605-3605.

5 H. David, Q. Fulian, F. John, X. Yanmeng, E. Peter, S. Darren, *Phys. Chem. Chem.Phys. Pccp,* 2013, **15,** 12215-12219.

6 K. Qi, Z. Jin, L. Xue, G. Zhu, X. Feng, Y. Ma, H. Wei, L. Jie, *Nano Energy,* 2016, **32,** 201-208.

7 F. Qiu, D. Harrison, J. Fyson, D. Southee, *Smart Science,* 2014, **2,** 107-115.

8 F. Yongping, C. Xin, W. Hongwei, L. Zhibin, H. Shaocong, P. Ming, Y. Xiao, Z. Dechun, *Adv. Mater.,* 2012, **24,** 5713-5718.

9 Z. Zhitao, C. Xuli, C. Peining, G. Guozhen, Q. Longbin, L. Huijuan, Y. Zhibin, B. Wenyu, L. Yongfeng, P. Huisheng, *Adv. Mater.,* 2014, **26,** 466-470.

10 L. Liu, Y. Yu, C. Yan, K. Li, Z. Zheng, *Nat. Commun.,* 2015, **6,** 7260-7269.

11 X. Chen, H. Lin, J. Deng, Y. Zhang, X. Sun, P. Chen, X. Fang, Z. Zhang, G. Guan, H. Peng, *Adv. Mater.,* 2015, **26,** 8126-8132.

12 W. Kai, Q. Meng, Y. Zhang, Z. Wei, M. Miao, *Adv. Mater.,* 2013, **25,** 1494-1498.

13 F. Su, X. Lv, M. Miao, *Small,* 2015, **11,** 854-861.